Regular and irregular motion: new mechanical results and fibre optics analogies

1983 J. Phys. A: Math. Gen. 16 3657

(http://iopscience.iop.org/0305-4470/16/15/031)

J. Phys. A: Math. Gen. **16** (1983) 3657–3673. Printed in Great Britain

Regular and irregular motion: new mechanical results and fibre optics analogies

A Ankiewicz and C Pask

Department of Applied Mathematics, Research School of Physical Sciences, Australian National University, Canberra, ACT 2600, Australia

Received 1 April 1983

Abstract. We present some new results concerning regular and irregular motions in classical systems. The origin and motivation for the work is to be found in fibre optics. We show that the equations describing ray paths in axially uniform optical fibres are mathematically equivalent to the classical mechanics of a particle moving in a two-dimensional potential U. The classification of rays in non-circular cross-section fibres is related to questions of integrability and the existence of regular motion in mechanical systems. The elliptic fibre leads to potentials $U(w)$ where $w^2 = x^2 + A^2y^2$ where A is a constant. It is conjectured that such potentials give rise to regular motion as revealed by a study of phase space trajectories, but the second invariant is unknown. The special case $U = w^q$ is studied in detail. These potentials belong to the wider class in which U is a homogeneous function of x and y, but not all potentials in that class give rise to regular motions.

1. Introduction

There is currently great interest in systems which are simply defined in classical mechanics but which exhibit complex and unexpected behaviour. A typical example is a particle moving in a plane under the influence of a potential; contrary to what the standard mechanics texts might lull us into believing, the equations are in general non-integrable and the motion of the particle in phase space often appears to be stochastic rather than following regular periodic orbits. (See the reviews by Berry (1978), Helleman (1980) and Whiteman (1977) for examples.) In this paper we introduce a new class of two-dimensional potentials which pose some interesting questions concerning the generation of chaotic motions.

This work is motivated by studies in fibre optics, as we explain in § 2. We shall demonstrate that, mathematically, the ray equations for light propagation along optical fibres are exactly equivalent to the two-dimensional mechanical problem. The distance z along the fibre plays the part of time, while the refractive index profile relates to the potential. The class of rays known as tunnelling leaky rays describe light which is not totally guided by the fibre, but which attenuates due to a radiation mechanism (Snyder and Mitchell 1974, Adams *et al* 1975, Stewart 1975). The existence of tunnelling rays depends on the fibre cross-sectional shape and is related to the question of integrable equations of motion and constants of motion in the analogous mechanical system. Tunnelling rays can affect the information carrying capacity of an optical fibre and are important when interpreting measurements (Ankiewicz and Pask 1978,

Adams *et al* 1976). It is the difficulty in the latter work when non-circular cross-section fibres are involved (Petermann 1977, Ramskov Hansen *et al* 1980, Barrell and Pask 1980) which leads us to apply techniques developed in classical mechanics.

The deviations from circularity immediately suggest the first-order distortion giving elliptical refractive index contours or equipotential curves. Thus we are led to mechanical problems with potentials of the form

$$U = U(x^2 + A^2y^2) \tag{1.1}$$

where x and y are cartesian coordinates in the plane and A is a constant equal to the ratio of the ellipses' semi-major to semi-minor axes.

The optimised optical fibre refractive index profile used in practical designs (Gloge and Marcatili 1973) has a power law behaviour and this leads to the specific potential form

$$U = (x^2 + A^2y^2)^{q/2} \tag{1.2}$$

where q is a constant. The advantage of these potentials is that we have mechanical similarity (see Landau and Lifshitz 1969, § 10) so that the behaviour of the orbits pertaining to one energy is also that for any other energy if a scaling transformation is applied. This contrasts with the classic Hénon and Heiles (1964) example which reveals strong energy-dependent characteristics.

In § 3 we give evidence to support our conjecture that potentials of the form in equation (1.2) lead to regular motions which indicate the existence of an integral of motion in addition to the energy. These results pose two further questions which we consider in §§ 4 and 5. The principle of mechanical similarity only requires U to be a homogeneous function of x and y, i.e. there is a q such that for any α

$$U(\alpha x, \alpha y) = \alpha^q U(x, y), \tag{1.3}$$

and it might be suspected that all homogeneous functions lead to orderly motions. On the other hand, the simple and symmetric form of the elliptical equipotential contours described by (1.1) leads us to ask whether all potentials of this form are integrable, with (1.2) just providing a special case.

The discussion forming § 6 should convey to the reader several challenges since one of our aims is to ask questions rather than just present a series of cut and dried results.

2. Optical and mechanical analogues

2.1. Basic formalism

An optical fibre is a cylindrical dielectric structure which we take to be uniform axially and aligned with the z axis. The refractive index $n(x, y)$ is greatest in the core region, which is surrounded by a cladding, usually assumed to be uniform. Following convention, we set

$$n^2(x, y) = n_0^2[1 - 2\Delta g(x, y)] \tag{2.1}$$

where n_0 is the maximum refractive index within the core and Δ is related to the cladding refractive index n_{cl} by

$$n_{cl}^2 = n_0^2(1 - 2\Delta). \tag{2.2}$$

The grading function g describes the variation of refractive index and

$$\begin{aligned} &0 \leqslant g(x, y) < 1 \qquad \text{in the core,} \\ &g(x, y) = 1 \qquad \text{in the cladding.} \end{aligned} \tag{2.3}$$

In practice the manufacturer aims to produce a circular cross-section fibre with a power law profile so that

$$g(x, y) = (x^2 + y^2)^{q/2} = r^q, \tag{2.4}$$

where we take $r = 1$ as the core boundary and q is a parameter chosen to optimise the fibre information carrying capacity (Gloge and Marcatili 1973, Olshansky and Keck 1976, Ankiewicz and Pask 1977). Note that throughout this paper all lengths are scaled and dimensionless, giving $g(x, y) = 1$ on the boundary.

We now follow the ray theory given by Ankiewicz and Pask (1977). The ray paths are given by Born and Wolf (1970, § 3.2)

$$(\mathrm{d}/\mathrm{d}s)(n\ \mathrm{d}\boldsymbol{R}/\mathrm{d}s) = \boldsymbol{\nabla} n \tag{2.5}$$

where $\boldsymbol{R}$ is the position vector for a point on the ray path and s is measured along the ray path, as shown in figure 1. For an axially uniform fibre, n is independent of z, and (2.5) gives

$$n\ \mathrm{d}z/\mathrm{d}s = n \cos\theta = \text{constant} \equiv \tilde{\beta}. \tag{2.6}$$

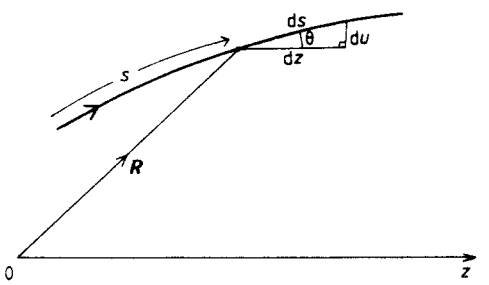

Figure 1. Ray path. A point on the path is $\boldsymbol{R} = (x, y, z)$ and s is the distance along the path. By geometry $\mathrm{d}z/\mathrm{d}s = \cos\theta$ and $(\mathrm{d}s)^2 = (\mathrm{d}z)^2 + (\mathrm{d}u)^2 = (\mathrm{d}x)^2 + (\mathrm{d}x)^2 + (\mathrm{d}y)^2$.

If we substitute (2.1) into (2.5) and use (2.6) to convert to z derivatives we obtain

$$(\tilde{\beta}^2/n_0^2\Delta)\mathrm{d}^2\boldsymbol{r}/\mathrm{d}z^2 = -\boldsymbol{\nabla} g(x, y). \tag{2.7}$$

We now set

$$t = n_0 z\, \Delta^{1/2}/\tilde{\beta} \tag{2.8}$$

and then (2.7) becomes

$$\mathrm{d}^2\boldsymbol{r}/\mathrm{d}t^2 = -\boldsymbol{\nabla} g(x, y) \tag{2.9}$$

where $\boldsymbol{r} = (x, y)$. This is readily recognised as mathematically equivalent to Newton's equation of motion for a particle of unit mass moving in a potential U identical with the refractive index grading function:

$$U = g(x, y). \tag{2.10}$$

The geometry of the path shown in figure 1 gives

$$(ds)^2 = (dz)^2 + (dx)^2 + (dy)^2 \tag{2.11}$$

which together with (2.6) leads to

$$n^2/\tilde{\beta}^2 = (dx/dz)^2 + (dy/dz)^2 + 1, \tag{2.12}$$

or, in terms of the (2.1) definition,

$$\tfrac{1}{2}(\tilde{\beta}^2/n_0^2\Delta)[(dx/dz)^2 + (dy/dz)^2] + g(x, y) = (n_0^2 - \tilde{\beta}^2)/2\Delta n_0^2. \tag{2.13}$$

We define the constant E by

$$E \equiv (n_0^2 - \tilde{\beta}^2)/2\Delta n_0^2 = (n_0^2 - \tilde{\beta}^2)/(n_0^2 - n_{cl}^2), \tag{2.14}$$

since in the mechanical analogy equation (2.13) is just the conservation of energy equation. We introduce the momentum

$$p_x = dx/dt = (\tilde{\beta}/n_0\sqrt{\Delta})\, dx/dz \tag{2.15}$$

and define p_y similarly. In ray optics p_x and p_y are related to angles made by the ray path. Equation (2.13) becomes

$$\tfrac{1}{2}(p_x^2 + p_y^2) + g(x, y) = \tfrac{1}{2}(p_x^2 + p_y^2) + U(x, y) = E. \tag{2.16}$$

We thus see that ray theory in fibre optics is exactly equivalent to two-dimensional classical mechanics. The projection of ray paths onto the fibre cross section (see Ankiewicz and Pask 1977, figure 4 for example) gives a curve $x(z)$, $y(z)$ which is just that traced out by a particle with unit mass moving in a plane under the action of the potential U and with energy E specified by (2.14).

2.2. Ray classification

Rays can be partially specified by the path constant $\tilde{\beta}$, which by definition (equation (2.6)) satisfies $\tilde{\beta} \leqslant n_0$. The first class of rays have $\tilde{\beta} > n_{cl}$ and hence $E < 1$. Equation (2.13) then requires that all points x, y on the ray path must give $g(x, y) < 1$ so that these points are all in the fibre core according to (2.3). The rays with $n_{cl} < \tilde{\beta} \leqslant n_0$ are thus totally confined to the core and are called bound or trapped rays.

The rays with $\tilde{\beta} < n_{cl}$ and $E > 1$ can always satisfy (2.13) with the straight line paths which occur in a uniform cladding. Rays launched in the core with $\tilde{\beta} < n_{cl}$ may reach the core–cladding boundary and hence join smoothly to a cladding path; these rays are not trapped in the fibre core but leave it by the refraction mechanism—see figure 2. However, some rays launched in the core may follow paths which do not reach the core–cladding boundary and thus there is no geometric link, consistent with the ray-specifying parameters such as $\tilde{\beta}$, to the ray paths in the cladding. This is analogous to a particle confined by a potential barrrier; classically the particle is trapped in that region but quantum mechanically it may tunnel through the barrier to follow one of the free space paths. Wave optics provides a similar result and ray paths confined to the core, but having $\tilde{\beta} < n_{cl}$, do not represent trapped power since they are connected to the external or cladding paths by an evanescent field. Each time the path goes through an outer turning point there is a portion of the power which leaks or tunnels into the cladding. This class of rays is called 'tunnelling' and is associated with power which is partially trapped within the fibre core but gradually

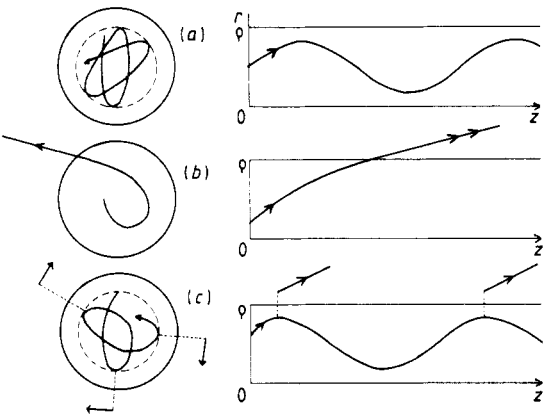

Figure 2. Schematic drawings of rays in a circular cross-section graded index fibre: (*a*) trapped, (*b*) refracting, (*c*) tunnelling ray. The broken circle marks the outer caustic and the broken line represents an evanescent field interaction connecting paths in the core and the cladding. The fibre has core radius ρ.

radiates away (Snyder and Mitchell 1974, Adams *et al* 1975, Stewart 1975, Ankiewicz and Pask 1978). See figure 2.

To complete the classification we need to know which initial conditions x_0, y_0, $(dx/dz)_0$, $(dy/dz)_0$, consistent with a given $\tilde{\beta} < n_{cl}$, lead to a path confined to the core when the initial point x_0, y_0 is in the core. It may be possible to do this if a second path constant is available, as we now demonstrate for circular cross-section fibres.

2.3. Circular cross-section fibres

In this case g depends only on the radial coordinates r, and consideration of azimuthal variations in (2.5) leads to the second ray path constant (Ankiewicz and Pask 1977)

$$\tilde{l} = r[n^2(r) - \tilde{\beta}^2]^{1/2} \cos\phi \tag{2.17}$$

where ϕ is the angle between the ray path projection onto the x, y plane and the azimuthal direction. Thus $\tilde{l}$ indicates the conservation of angular momentum, $xp_y - yp_x$. We find it convenient to use a normalised second invariant (Hartog *et al* 1982) $\Lambda = \tilde{l}^2/(2\Delta n_0^2)$. Ray paths are now completely labelled by $\tilde{\beta}$ and $\tilde{l}$ (or E and Λ), and the class of tunnelling rays can be specified. For example, for the power law fibres (see equation (2.4)) Ankiewicz and Pask (1977) show that tunnelling rays have

$$1 \leqslant E \leqslant \min(1 + q/2,\ 1/2\Delta), \tag{2.18}$$

$$E - 1 \leqslant \Lambda \leqslant \tfrac{1}{2}q[2E/(q+2)]^{1+2/q}. \tag{2.19}$$

The initial conditions are used to find E and Λ and the ray type is then immediately known: if $E < 1$, the ray is trapped; if $E > 1$ and Λ satisfies (2.19) the ray is tunnelling; if $E > 1$ and (2.19) is not satisfied, the ray is refracting.

2.4. Remaining problems and mechanical questions

For non-circular cross-section fibres, $\tilde{l}$ is no longer a constant and in general the ray equation does not readily reveal a second constant. It is obvious that $\tilde{l}$ corresponds

to angular momentum in the analogous mechanical system established in § 2.1. We can now also appreciate the link between the problem of finding which rays show a tunnelling behaviour and the search for integrable equations and constants of motion in mechanical problems with non-central forces.

The first-order distortion of cross section might be expected to lead to elliptical shapes rather than circles so that (2.4) is replaced by

$$g(x, y) = (x^2 + A^2 y^2)^{q/2} \tag{2.20}$$

where $A \neq 1$ implies elliptical iso-indicial contours. The identification of g with potential U in (2.10) then leads to potentials (1.1), (1.2) and (1.3), as discussed in the introduction.

Thus the rest of this paper is concerned with the motion of a particle in some very simple but important two-dimensional potentials and the search for regular motion and integration constants. The motivation has been spelled out in this section and the reader may reinterpret all mechanical results in terms of ray paths in an optical fibre.

3. Motion in elliptical power-law potentials

3.1. General formalism

We consider a particle moving in a plane so that the Hamiltonian H is

$$H = \tfrac{1}{2}(p_x^2 + p_y^2) + U(x, y). \tag{3.1}$$

For a conservative system $H = E$ provides a first integral and the problem is reduced to quadratures if a second integral μ exists,

$$f(x, y, p_x, p_y) = \text{constant} = \mu. \tag{3.2}$$

Knowledge of E and μ provides bounds on the parts of phase space available to a particle and, in particular, the regions of configuration space x, y which may be reached; this is the information required in the ray classification problem discussed in § 2.

The search for μ may be carried out mathematically or numerically. The mathematical approach usually relies on the exploitation of some symmetry or choice of variables leading to a separable problem—we give examples in §§ 3.2, 3.3 and 4.2 and return to the point again in the discussion.

In the numerical approach, initial conditions are chosen and $x(t)$, $y(t)$, $p_x(t)$ and $p_y(t)$ are computed using a series of steps in time. The relation $H = E$ means that only three of the four phase space variables are independent, e.g. x, y, p_x. If the motion is irregular the volume available in x, y, p_x space will be filled with quasi-random motions and any plane cut through this volume will show a scattering of irregular points as the particle phase space trajectory cuts through it. However, if the second integral exists, a plane, such as the x, p_x plane for $y = 0$, will reveal a smooth curve filled in by the points generated each time the trajectory passes $y = 0$. This method is beautifully introduced by Hénon and Heiles (1964) and in the textbook by Park (1979), and is discussed extensively by Berry (1978) and Helleman (1980). This approach is applied in §§ 3.4, 4.1 and 5.

We now consider details for power law elliptical potentials as in equation (1.2).

3.2. Special case: parabolic potential profile

In this case $q = 2$ and the Hamiltonian (3.1) separates:

$$H = \tfrac{1}{2}p_x^2 + x^2 + \tfrac{1}{2}p_y^2 + A^2y^2 \tag{3.3}$$

$$= H_1(x, p_x) + H_2(y, p_y) \tag{3.4}$$

and the x and y motions are independent, except that their energies satisfy $E_2 = E - E_1$. This gives the two integrals of motion E and E_1. In the fibre optics context, this case is discussed by Ankiewicz (1979a) and Barrell and Pask (1979). Whenever the grading function $g(x, y)$ (equation (2.1)), and hence the equivalent potential $U(x, y)$, separates into a function of x plus a function of y the second invariant allows us to prove that no pure tunnelling rays can exist since eventually any non-bound ray reaches the core–cladding boundary and escapes by refraction.

3.3. Special case: the step profile with elliptical boundary

This case corresponds to taking $q \to \infty$ in (1.2) and we have a uniform elliptically shaped region with boundaries which reflect particles or rays. Within this region the particle or ray paths are straight lines and the standard process with equal angles of incidence and reflection occurs at the boundary. For this case the second invariant μ does exist:

$$\mu = (xp_y - yp_x)^2 - p_y^2(1 - A^{-2}), \tag{3.5}$$

as we prove in the appendix, where we show that μ is in fact the product of the angular momenta taken about the two focal points of the elliptical boundary. Berry (1981) has given this invariant in terms of angles and distance around the elliptical boundary. Clearly, as the potential contours become circular, $A \to 1$ and μ reduces to the conventional angular momentum squared.

The possible paths consistent with a given E ($= [p_x^2 + p_y^2]/2$ in this case) must have μ satisfying

$$-2E(1 - A^{-2}) < \mu < 2E/A^2 \tag{3.6}$$

and the regions of x, y space available to such paths can also be classified, leading to the caustics in the optical problem. There are two types of ray congruences: the paths with positive μ generate an inner caustic which is an ellipse confocal with the boundary; the paths with $\mu < 0$ have no inner caustic but lie in a region bounded by a hyperbola and the interface. Pure tunnelling rays are found only in the $\mu > 0$ class. For further details of the fibre optics applications, see Ankiewicz (1979a) and Love *et al* (1979).

We can use the angle relations given in the latter paper to indicate the various types of rays in terms of their invariants. One difference from the circular case is that there is a new class of 'slowly refracting' or 'tunnelling/refracting' rays—these tunnel for a while, but at some point along the fibre they refract. They are in the range

$$2(EA^{-2} - 1) < \mu < 2A^{-2}(E - 1), \qquad E > 1.$$

Refracting rays have

$$\mu < 2(EA^{-2} - 1)$$

whilst the 'pure' tunnelling ones have

$$2A^{-2}(E - 1) < \mu < 2EA^{-2}.$$

The maximum possible value of E is $1/2\Delta$. By comparing the $q \to \infty$ limit of (2.19) with the $A \to 1$ limit here, we see that μ is identified with 2Λ.

We now turn to the phase space trajectories and in particular those curves in the x, p_x plane which correspond to a given E and $y = 0$. In the present case the numerical approach outlined in § 3.1 is unnecessary since equation (3.5) with $y = 0$ and $p_y^2 = 2E - p_x^2$ gives

$$(x^2 - 1 + A^{-2})(2E - p_x^2) = \mu. \tag{3.7}$$

Contours for constant μ are plotted in figure 3. The contour for $\mu = 0$ corresponds to the vertical lines

$$x \equiv x_v(\infty) = \pm F \tag{3.8}$$

where $F^2 = 1 - A^{-2}$ and the focal points of the ellipse forming the boundary are at $(\pm F, 0)$. Obviously if a path goes through either focus it has zero angular momentum about that point and μ is zero since it is the product of the angular momenta taken about the two foci.

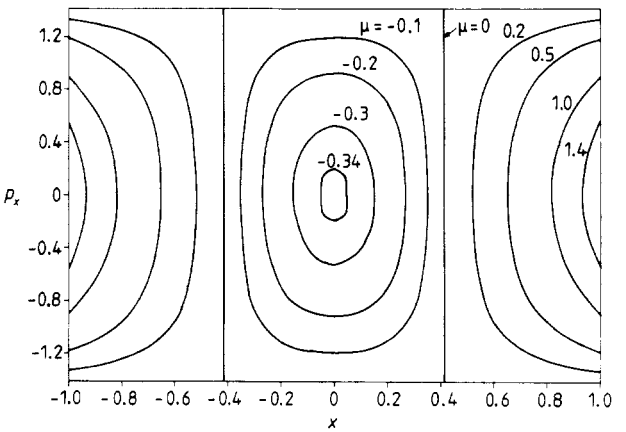

Figure 3. The x–p_x phase diagram for $y = 0$ in a step profile potential with elliptical boundary. A curve can be labelled by its μ value and intersects the x axis at $(F^2 + \mu/2E)^{1/2}$; if $\mu < 0$ it intersects the p_x axis at $(2E + \mu/F^2)^{1/2}$. Here $A = 1.1$ and $E = 1$.

3.4. Numerical studies

For the general elliptical power law potential as in (1.2), with $q \neq 2$ or ∞, we must resort to the numerical approach outlined in § 3.1. For a specified E, we use a computer program to trace out the particle trajectory, or ray path, numerically and store values of x and p_x each time the trajectory crosses the $y = 0$ plane. By superimposing results for various initial conditions we can build up a portrait covering the x, p_x plane for a given E and find how much of the plane is covered by smooth curves (cross sections of tori). The coupled differential equations to be solved numerically are

$$d^2x/dt^2 = -qx[x^2 + A^2y^2]^{(q-2)/2}, \tag{3.9}$$

$$d^2y/dt^2 = -qAy[x^2 + A^2y^2]^{(q-2)/2}. \tag{3.10}$$

As mentioned in the introduction, the potentials in (1.2) also satisfy equation (1.3), i.e. they are homogeneous functions of degree q. Therefore the principle of mechanical similarity holds (Landau and Lifshitz 1969, § 10) and the paths for different energies differ only by scaling factors. (This fact has been exploited in fibre optics by Barrell and Pask (1980) and Pask (1979).) Thus, if a given profile (A, q) exhibits no stochastic behaviour for some value of E, then there will be no stochastic behaviour for all values of E. In general, one would expect a mixture of regular and stochastic patterns. To our surprise, we found no evidence of stochastic behaviour for any combination of A and q. For fibres we are mainly concerned with $A < 1.2$, but we studied examples with A as high as 10 and always found completely regular behaviour. The fact that the x, p_x plane is covered with smooth curves gives strong evidence for the existence of a second invariant, μ, for all these profiles. This is in contrast to the Hénon–Heiles potential, and the profiles to be studied in § 4.1. It is not known at the present time whether this invariant can be expressed in terms of elementary functions.

The x–p_x plots take three different forms, depending on A, and whether q is low, close to 2, or high. These regions are defined by

$$\text{region 1:} \quad q > q_d(A), \tag{3.11}$$

$$\text{region 2:} \quad q_l(A) < q < q_d(A), \tag{3.12}$$

$$\text{region 3:} \quad q < q_l(A), \tag{3.13}$$

and examples of all three are given in figure 4. Since scaling applies, we have used $E = 1$ in all these plots. Each curve would represent a different value of a second invariant μ.

There are two values of x which are of particular interest when interpreting the phase space plots in figure 4: the fixed points x_F which represent the cases where the x–p_x curves have shrunk to a single point, and the transition points x_v which divide the x axis into regions crossed by curves of different types. These values depend on the potential parameters A and q (equation (1.2)).

When $q = \infty$, $x_F = 1$; as q decreases, so does x_F, reaching a minimum at $q = q_m$, and then increasing again and meeting the interface $(x_F = 1)$ at $q = q_d(A)$. An example of this region 1 behaviour is shown in figure 4(a). When q is in region 2 (equation (3.12)), which we show below means q near 2, patterns such as those in figure 4(b) occur and there are no fixed points, apart from (0, 0). Thus all orbits come arbitrarily close to $(x, y) = (0, 0)$ and so no inner caustics exist. As q decreases below $q_l(A)$, a new pattern emerges, with x_F increasing (from 0) with decreasing q; the 'figure of eight' loop crosses the x axis at $x_v(q)$. An example of this region 3 behaviour is given in figure 4(c). Table 1 gives some of the values of q_l, q_d and q_m, ascertained numerically, for various values of A. In fibre optics we are generally concerned with ellipticities of not more than 10 or 20% (i.e. $A < 1.2$), and it will be observed that for these values we have the approximations

$$q_l(A) \simeq 2/A, \tag{3.14}$$

$$q_d(A) \simeq 2A. \tag{3.15}$$

If we had chosen to investigate the curves in the y, p_y plane obtained when $x = 0$ we would obtain y_F and y_v. The results for x_F, x_v, y_F and y_v are plotted in figures 5 and 6. These results are for $E = 1$, but the scaling property for these potentials

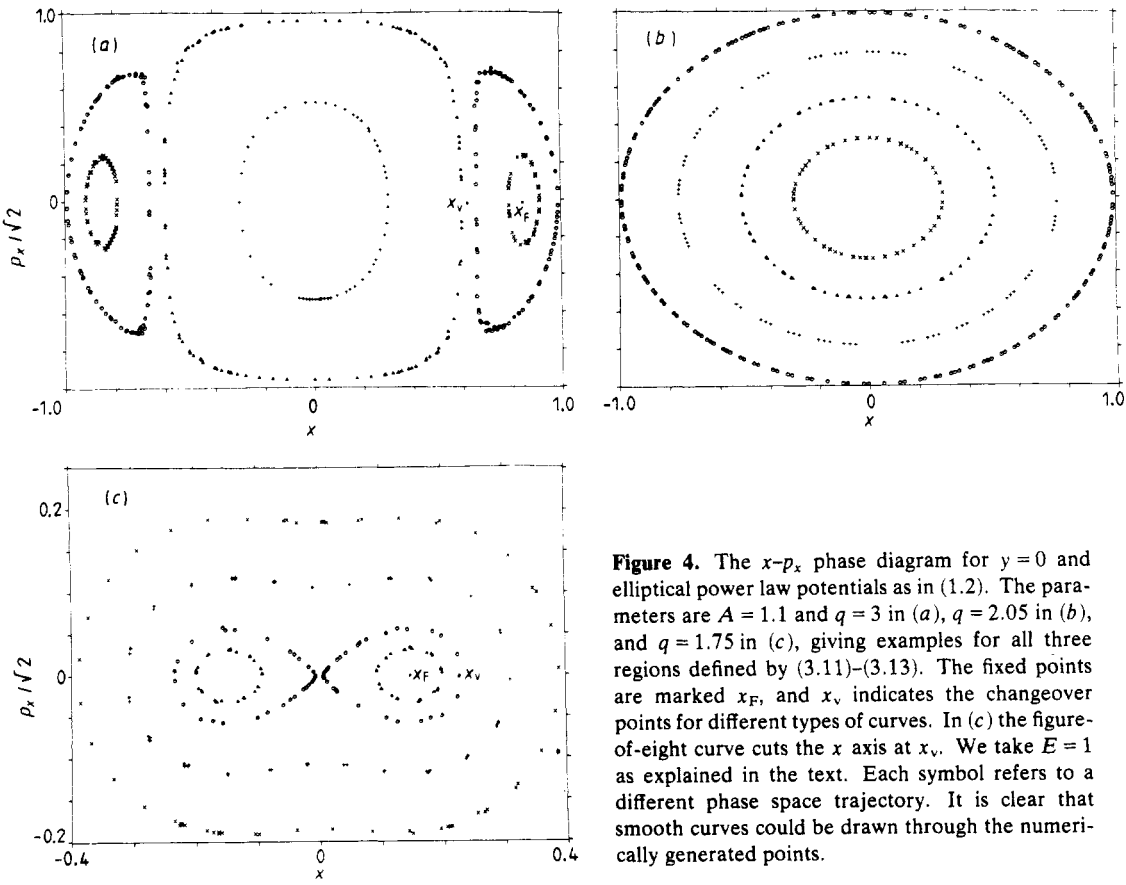

Figure 4. The x–p_x phase diagram for $y = 0$ and elliptical power law potentials as in (1.2). The parameters are $A = 1.1$ and $q = 3$ in (a), $q = 2.05$ in (b), and $q = 1.75$ in (c), giving examples for all three regions defined by (3.11)–(3.13). The fixed points are marked x_F, and x_v indicates the changeover points for different types of curves. In (c) the figure-of-eight curve cuts the x axis at x_v. We take $E = 1$ as explained in the text. Each symbol refers to a different phase space trajectory. It is clear that smooth curves could be drawn through the numerically generated points.

Table 1. Critical exponents q for various A.

A	q_l	q_d	q_m
1.02	1.96	2.04	3
1.05	1.905	2.105	4
1.1	1.825	2.21	4.5
1.15	1.75	2.32	5.5
1.2	1.685	2.435	6

(Landau and Lifshitz 1969, § 10) means that

$$x_F(A, q, E) = E^{1/q} x_F(A, q, 1) \tag{3.16}$$

and similarly for x_v, y_F and y_v.

We note here that the completely regular behaviour generated by these potentials is quite atypical amongst the total class of mechanical systems, and non-integrability appears to be the rule (Helleman 1980). For this reason we investigate the properties of potentials as in equation (1.2) which may be responsible for this special feature. The existence of a second invariant indicates some 'hidden symmetry' (Moser 1980), but there is no standard way to find it.

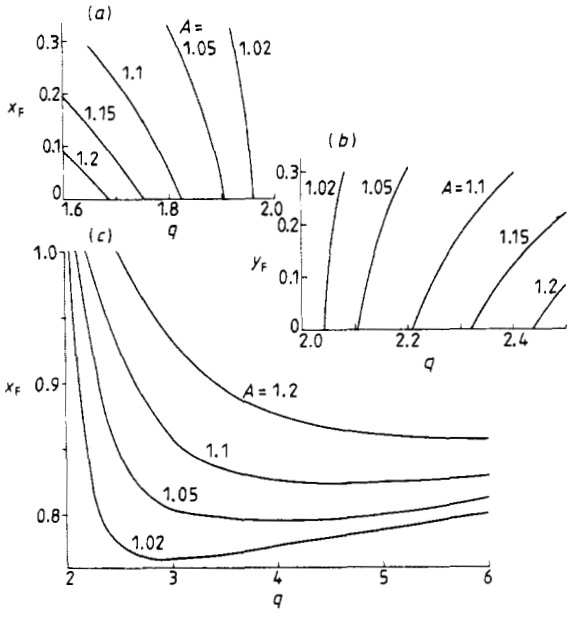

Figure 5. (*a*) Location of x_F ($q<2$) (using the $y=0$ slice giving the x–p_x plane). The intercepts on the q axis give $q_l(A)$. (*b*) Position of y_F (using the $x=0$ phase space slice to give the y–p_y plane) for $q>2$. The intercepts on the q axis give $q_d(A)$. (*c*) x_F for $q>2$. At the intersection of the curves with the line $x_F=1$ we have $q=q_d(A)$; the same values of $q_d(A)$ are obtained from (*b*). As A increases, so does q_m, the position of minimum x_F; as $q\to\infty$ we have $x_F\to 1$ for all curves.

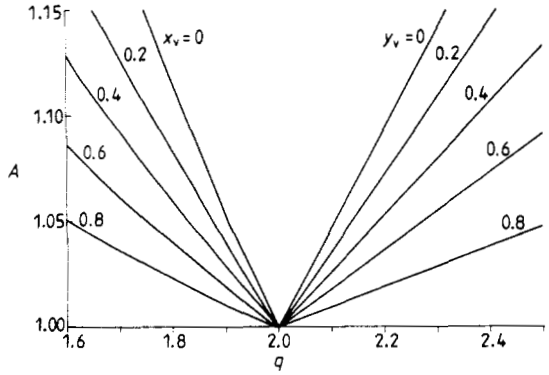

Figure 6. Lines of constant x_v and y_v. The $x_v=0$ line is $A=2/q$, and the $y_v=0$ line is $A=2q$. For $q>2$ and below the $y_v=0$ line a very good approximation is $y_v=1-2.16(A-1)/(q-2)$.

3.5. Optical consequences

If a single mode is launched into a multimode fibre, then the intensity pattern observed at the end depicts the mode field, or equivalently the ray congruence formed from the ray path projection on the cross section. Consider a curve for a given value of μ on any of the diagrams in figures 3 and 4. We can deduce two types of behaviour.

The first type corresponds to x–p_x curves which are single closed loops and these are found in the central regions of figures 3 and 4(a), in figure 4(b), and in the outer regions of figure 4(c). Each time $y = 0$, (x, p_x) is somewhere on such a loop. This means that all values of $|x|$ from 0 to some maximum occur, and that the (x, y) ray congruence cannot have an inner caustic; the light intensity near the fibre centre is thus high for these $(\tilde{\beta}, \mu)$ modes. These 'hyperbolic' modes cannot be tunnelling; their actual shapes are given by Ankiewicz (1979a). Note that figure 4(b) corresponds to region 2 q-values (equation (3.12)) which means near-parabolic ($q = 2$) fibres, according to the bounds in table 1. Thus, in fibres with elliptical contours which are sufficiently close to the parabolic profile all modes are of 'hyperbolic' type.

The second type of behaviour relates to the part of figure 4(c) within the 'figure of eight', the $|x| > F$ part of figure 3 and the large $|x|$ part of figure 4(a). Each constant μ curve now consists of two disjoint parts. Each time $y = 0$, $|x|$ is between two values which can be read off the x axis, and it is never close to zero. Thus an inner caustic exists and the intensity pattern will be qualitatively different from those of the modes discussed above. In particular, the intensity near the centre will be very low. These 'elliptic' modes can be bound or tunnelling; for fixed eccentricity the proportion of 'elliptic' modes will increase as $|q - 2|$ increases (Ankiewicz 1979b)—see figure 6.

When μ reaches its limiting value for the 'elliptic' congruences, the two separate loops in the (x, p_x) plane shrink to points, located at $(\pm x_F, 0)$—see figures 4(a) and (c). If the ray's initial condition is $x_0 = x_F$, $(p_x)_0 = 0$, then $x = \pm x_F$ each time $y = 0$, and the congruence reduces to a single closed curve in the (x, y) plane. Thus, in the phase plots, each fixed point corresponds to a closed periodic orbit in the fibre cross section—this means that the inner and outer caustics coalesce.

There has been considerable theoretical and experimental work reported for elliptical fibres, and apart from those already cited we mention Ankiewicz *et al* (1979), Yevick and Stolz (1980), Checcacci *et al* (1980), Brenci *et al* (1981) and Saijonmaa *et al* (1982).

4. Homogeneous function potential

4.1. General question

The results presented in § 3 may induce one to surmise that all homogeneous potentials lead to regular behaviour. This is not the case, as we now show with a counterexample. We consider

$$U = (x^4 + A^4 y^4)^{q/4}. \tag{4.1}$$

This class satisfies scaling property (1.3), so we may again take $E = 1$ without loss of generality. The topology of the orbits is now quite complicated, and it features both regular and stochastic behaviour. An example is given in figure 7. All the points marked by triangles are generated by a single trajectory.

4.2. Special cases

While potential (4.1) provides a counterexample to the general proposition, it does not mean that the elliptic power-law potentials (1.2) are the only homogeneous function potentials leading to regular behaviour. We next offer two other examples.

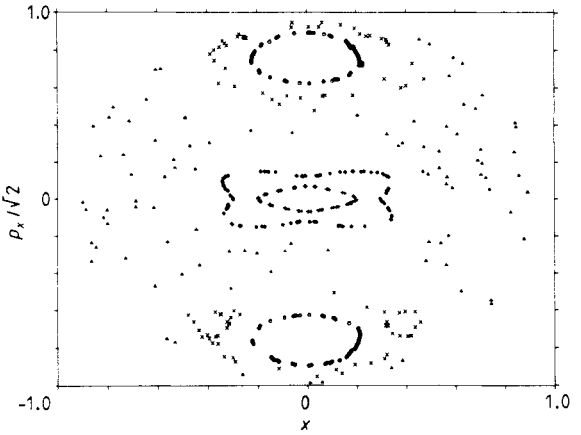

Figure 7. x–p_x plot for $y = 0$ and $E = 1$ and potential of form (4.1). Here $A = 1.1$ and $q = 1.9$. Each symbol refers to a different phase-space trajectory. It is clear that part of the area is covered by a stochastic region.

Whenever $U(x, y)$ is a separable function of x and y, the Hamiltonian separates as in (3.4), and a second invariant exists, since the x and y motions have their own conserved energies. This will lead to a regular phase space curve. Therefore, for any constants C_1 and C_2,

$$U(x, y) = C_1 x^q + C_2 y^q \tag{4.2}$$

is a homogeneous function of degree q which leads to regular mechanical behaviour.

Potentials which are separable in other coordinate systems also lead to a second invariant, and as a second example we consider parabolic cylindrical coordinates. In this case we obtain a separable problem when (Landau and Lifshitz 1969, § 48)

$$U(x, y) = [g(r + x) + h(r - x)]/r \tag{4.3}$$

where $r^2 = x^2 + y^2$. If we now take

$$g(u) = C_1 u^{q+1}, \qquad h(u) = C_2 u^{q+1}, \tag{4.4}$$

we again obtain a potential which is homogeneous of degree q and generates regular mechanical behaviour. In terms of polar coordinates r, θ we can write (4.3) as

$$U = [r/\rho(\theta)]^q \tag{4.5}$$

where ρ is the radius depending on angle according to

$$\rho(\theta) = C_1(1 + \cos\theta)^{q+1} + C_2(1 - \cos\theta)^{q+1}. \tag{4.6}$$

There is one major difference between these examples and the potentials (1.2): the latter potentials have elliptical potential contours for any value of q, but the potentials in (4.2) and (4.5) have contours which vary as q varies. This underlines the point that these examples have special mathematical forms which lead to integrable equations of motion.

5. Potentials with elliptical contours

It seems that the concentric ellipse form of potential contours may provide the clue to the regular behaviour and integrability reported in § 3. To investigate this further we consider potentials of the type

$$U = U(w) \tag{5.1}$$

where

$$w = (x^2 + A^2 y^2)^{1/2}. \tag{5.2}$$

Obviously scaling does not apply for these potentials. There is an unlimited number of forms for $U(w)$, so a mathematical proof would be required to make a general statement concerning regular trajectories for all energies in this class of profiles. Lacking such a proof we report some numerical results.

Take

$$U = (2\Delta)^{-1} \tanh^2(\sqrt{2\Delta}w). \tag{5.3}$$

Using (2.1) and (2.10), we see that this corresponds to a fibre with a refractive index which is of considerable interest in fibre optics:

$$n^2 = n_0^2 \operatorname{sech}^2(\sqrt{2\Delta}w). \tag{5.4}$$

From numerical results, the behaviour seems completely regular, and virtually the same as that for a parabolic fibre with concentric ellipse index contours.

We also examined cases with a fourth-order term (w^4). We set $U(1) = 1$ and so take

$$U(w) = w^2(1 + Cw^2)/(1 + C) \tag{5.5}$$

where C is a constant. Our computer studies again indicate regular behaviour and indeed, given C and A, one can find a power-law ellipse exponent q which gives a similar phase plot. We did not observe any onset of stochasticity. For C negative, the x–p_x plots resemble the figure 4 plots for q low (< 2), while those for C positive (e.g. $C = +1$) are like those for high values of q.

These numerical results should be taken as suggestive, and perhaps the best we can say is that we have not come across a counterexample to our conjecture that potentials of the form (5.1) lead to regular mechanical behaviour.

6. Discussion

The approach of topological dynamics has been used to explain phenomena in various branches of physics, such as plasmas, galactic motion and the beam–beam interaction; we believe this is the first application of such concepts to explain propagation of light in optical fibres. We have related results to ray caustics, observed intensity patterns and critical values of exponents in multimode fibre investigations.

The application of methods of topological dynamics to potentials which are homogeneous functions of x and y has the advantage that only one energy value need be considered, since scaling and mechanical similarity preclude the onset of irregular behaviour at some particular energy. While not all such functions give rise to regular behaviour, it does appear that the power law potentials, equation (1.2), represent

a new, large class of integrable systems. This is of importance in fibre optics, because it implies the existence of tunnelling rays in many non-circular fibres, but it is also interesting theoretically since integrable systems are known to be rare in the totality of all Hamiltonians (Helleman 1980).

It is also interesting to note that Richstone (1982) explored galactic motion using a potential with pronounced scaling properties and found that the phase space behaviour is always regular, in contrast to the variety of irregularities found by Hénon and Heiles (1964) in their classic study of that astrophysical subject.

The second invariant is most easily found for systems which can be made separable with a suitable choice of coordinates (Landau and Lifshitz 1969, § 48), but this method does not apply in the present case. A second approach is to pick a form for the invariant and then work backwards to the possible potential (Holt 1982, Whittaker 1927), but again this has not proved possible in our case. There does not appear to be a general method for detecting regular systems, and those Hamiltonians which have been integrated (e.g. the Toda lattice) seem to depend on mathematical quirks peculiar to them. It has been conjectured that integrability is related to the 'Painlevé condition' involving singularities of differential equations in the complex plane. The exploitation of this seems promising (Chang *et al* 1981, Bountis and Segur 1982), but the idea has yet to be put on a sound footing.

The Kolmogorov–Arnold–Moser (KAM) theorem (Berry 1978, Helleman 1980, Whiteman 1977) shows that when an integrable system is perturbed slightly, many of the phase space invariant tori still remain. In our case, this means that when A in equation (1.2) differs only slightly from unity, i.e. when we are very close to a central force system, then we expect mostly regular behaviour. This also suggests that we try in every case to find a known integrable system near to the present one and this approach was used by Ankiewicz (1979b). He used elliptical coordinates and found a separable potential (Landau and Lifshitz 1969, § 40) which approximated the potential in (1.2). The invariant generated by the approximation potential is not an exact invariant for the cases studied in this paper, but in some parameter regions it remains reasonably constant.

Appendix

Part of the path of a particle moving in a uniform potential region with a perfectly reflecting elliptical boundary is shown in figure 8. At a reflection the momentum $\boldsymbol{p}$ is changed in direction but not in magnitude, and between reflections the paths are straight lines. Consider l_1, the angular momentum taken about focal point 1 before the reflection:

$$l_1 = |\boldsymbol{r}_1 \times \boldsymbol{p}| = r_1 p \sin\theta = R_1 p \tag{A1}$$

where R_1 is the perpendicular from focal point 1 onto the path, $r_1 = |\boldsymbol{r}_1|$ and $p = |\boldsymbol{p}|$. Similarly for angular momenta about focal point 2 and for the path after reflection (referred to by primed quantities):

$$l_1' = R_1' p', \tag{A2}$$

$$l_2 = R_2 p, \tag{A3}$$

$$l_2' = R_2' p'. \tag{A4}$$

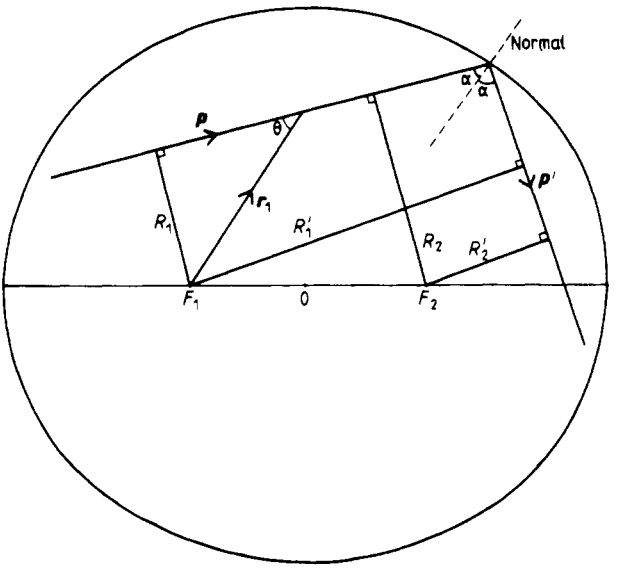

Figure 8. A reflection at a perfectly reflecting elliptical boundary. The focal points are F_1 and F_2 and R_1, R_1', R_2, R_2' are normals from the paths to the focal points. The momenta $\boldsymbol{p}$ and $\boldsymbol{p}'$ are directed along the paths.

By reflection law, $p = p'$, and a theorem in Euclidean geometry (Salmon 1855) asserts that

$$R_1R_2 = R_1'R_2'. \tag{A5}$$

These two facts, together with equations (A1)–(A4), imply that

$$l_1l_2 = l_1'l_2'. \tag{A6}$$

Since both l_1 and l_2, and hence l_1l_2, are constant for straight line paths and the product is unchanged by a reflection we conclude that

$$\mu = l_1l_2 \tag{A7}$$

is an invariant. The boundary is $x^2 + A^2y^2 = 1$ so that the focal points are $(\pm F, 0)$ with $F = (1 - A^{-2})^{1/2}$. Since $\boldsymbol{r}_1 = (x + F, y)$ and $\boldsymbol{r}_2 = (x - F, y)$ we find

$$l_1 = |\boldsymbol{r}_1 \times \boldsymbol{p}| = (x + F)p_y - yp_x, \tag{A8}$$

$$l_2 = |\boldsymbol{r}_2 \times \boldsymbol{p}| = (x - F)p_y - yp_x, \tag{A9}$$

which we substitute into (A7) to get

$$\mu = (xp_y - yp_x)^2 - p_y^2(1 - A^{-2}) \tag{A10}$$

$$= l^2 - p_y^2(1 - A^{-2}). \tag{A11}$$

In (A11) l is the angular momentum referred to the origin.

References

Adams M J, Payne D and Sladen F M E 1975 *Electron. Lett.* **11** 238–40
—— 1976 *Opt. Commun.* **17** 204–9
Ankiewicz A 1979a *Opt. Quant. Electron.* **11** 197–203
—— 1979b *Opt. Quant. Electron.* **11** 525–39
Ankiewicz A, Adams M J and Parsons N J 1979 *Opt. Lett.* **4** 414–6
Ankiewicz A and Pask C 1977 *Opt. Quant. Electron.* **9** 87–109
—— 1978 *Opt. Quant. Electron.* **10** 83–93
Barrell K F and Pask C 1979 *Opt. Quant. Electron.* **11** 237–51
—— 1980 *Electron. Lett.* **16** 532–4
Berry M V 1978 *Regular and Irregular Motion in Topics in Nonlinear Dynamics, AIP Conf. Proc.* 46 (New York: AIP) 16–120
—— 1981 *Eur. J. Phys.* **2** 91–102
Born M and Wolf E 1970 *Principles of Optics* 4th edn (Oxford: Pergamon)
Bountis T and Segur H 1982 *Mathematical Methods in Hydrodynamics and Integrability in Dynamical Systems, AIP Conf. Proc.* 88 (New York: AIP) 279–91
Brenci M, Checcacci P F, Falciai R and Scheggi A M 1981 *Radio Sci.* **16** 535–40
Chang Y F, Tabor M, Weiss J and Corliss G 1981 *Phys. Lett.* **85A** 211
Checcacci P F, Falciai R and Scheggi A M 1980 *J. Opt. Soc. Am.* **70** 1551–4
Gloge D and Marcatili E A J 1973 *Bell Syst. Tech. J.* **52** 1563–78
Hartog A H, Adams M J, Sladen F M E, Payne D N and Ankiewicz A 1982 *IEEE Quantum Electron.* **QE-18** 825–38
Helleman R H G 1980 *Self-generated chaotic behaviour in nonlinear mechanics* in *Fundamental Problems in Statistical Mechanics* V ed E G D Cohen (Amsterdam: North-Holland)
Hénon M and Heiles C 1954 *Astron. J.* **69** 73–9
Holt C R 1982 *J. Math. Phys.* **23** 1037–46
Landau L D and Lifshitz E M 1969 *Mechanics* (Oxford: Pergamon)
Love J D, Pask C and Winkler C 1979 *IEEE Microwaves, Optics and Acoust.* **3** 231–8
Moser J 1980 in *Dynamical systems, Prog. Maths.* vol 8 (Boston and Basel: Birkhäuser) pp 233–89
Olshansky R and Keck D B 1976 *Appl Opt.* **15** 483–91
Park D 1979 *Classical Dynamics and Its Quantum Analogues* (Berlin: Springer)
Pask C 1979 *J. Opt. Soc. Am.* **69** 1599–603
Petermann K 1977 *Electron. Lett.* **13** 513–4
Ramskov Hansen J J, Ankiewicz A and Adams M J 1980 *Electron. Lett.* **16** 94–6
Richstone D O 1982 *Astrophys. J.* **252** 496–507
Saijonmaa J, Halme S J and Yevick D 1982 *Opt. Quantum Electron.* **14** 225–36
Salmon G 1855 *Conic Sections* (London: Longmans) § 194 (p 166)
Snyder A W and Mitchell D J 1974 *J. Opt. Soc. Am.* **64** 956–63
Stewart W J 1975 *Electron. Lett.* **11** 321–2
Whiteman K J 1977 *Rep. Prog. Phys.* **40** 1033–69
Whittaker E T 1927 *A treatise on the analytical dynamics of particles and rigid bodies* (Cambridge: CUP)
Yevick D and Stoltz B 1980 *Electron. Lett.* **16** 210–1